We are IntechOpen,
the world's leading publisher of
Open Access books
Built by scientists, for scientists

6,900
Open access books available

186,000
International authors and editors

200M
Downloads

Our authors are among the

154
Countries delivered to

TOP 1%
most cited scientists

12.2%
Contributors from top 500 universities

CLARIVATE ANALYTICS
BOOK CITATION INDEX
INDEXED

WEB OF SCIENCE™

Selection of our books indexed in the Book Citation Index
in Web of Science™ Core Collection (BKCI)

Interested in publishing with us?
Contact book.department@intechopen.com

Numbers displayed above are based on latest data collected.
For more information visit www.intechopen.com

Chapter

Study of Electromagnetic Radiation Sources Using Time Reversal: Application to a Power Electronic Converter

Sassia Hedia, Bessem Zitouna,
Jaleleddine Ben Hadj Slama and Lionel Pichon

Abstract

Recently, modern power electronic systems have been introduced in different applications, such as in avionics and wireless communication. The increasing technological complexity of these systems is posing serious challenges regarding electromagnetic compatibility (EMC) issues. Indeed, the radiation emitted from electronic circuits can induce harmful effects on nearby devices. Thus, several research works have been conducted using the nearfield technique to deal with electromagnetic interferences (EMI) that might occur, especially due to rapidly changing currents and voltages. In the present work, a detailed study about the characterization of the electromagnetic nearfield-radiated emissions is established using a time-domain analysis to provide an equivalent model constituted of a set of electromagnetic dipole parameters. Source reconstruction has been obtained using electromagnetic time reversal (EMTR), which has proven successful and efficient in identifying transient disturbance sources in power electronics. Experimental measurements of the magnetic nearfield have been carried out under an AC/DC flyback converter. The accuracy of the proposed method has been confirmed by visualizing measured magnetic field components, which are in good agreement with the calculated maps. The results of a reasonable computing time have shown that, particularly in transient signals with a wide frequency band, the suggested inverse method is an adequate alternative to overcome frequency domain limitations.

Keywords: electromagnetic compatibility (EMC), electromagnetic time reversal (EMTR), nearfield, power electronics, radiated emissions, time-domain analysis

1. Introduction

In any electronic circuit, designers face serious challenges to ensure product efficiency and make it fit into a large community of electronic systems where harmful interferences can occur. Indeed, electromagnetic compatibility aims to achieve a peaceful coexistence of electronic equipment, especially when subjected to severe electromagnetic disturbances. In recent high-density PCBs (printed circuit boards), components are becoming increasingly sensitive to unwanted phenomena,

such as radiated and conducted emissions characterized by sudden variations in voltage and current [1, 2]. Thus, EMC researchers and engineers have conducted multiple works using various relevant approaches to predict these emissions with a reasonable tradeoff between guaranteeing a good accuracy and a reduced computing time. For instance, to deal with radiated emissions, authors in [3–5] have proposed to use matrix inversion methods that have ended up with a need for a large set of measurements. As a solution, hybrid optimization methods based on artificial intelligence techniques such as genetic algorithms (GA) and artificial neural networks (ANN) have been progressively introduced [6, 7], and this has contributed considerably to speed up the algorithm convergence at a fixed operating frequency.

The common point in the research mentioned above has been using the frequency domain (FD) to model electromagnetic fields through a set of equivalent dipoles [2–8]. To obtain a behavioral model of the device under test (DUT), particularly in power circuits of a fast switching nature [2, 5], a direct alternative way of proceeding is to perform measurements in the time domain (TD), which can also recover the frequency spectrum using a further signal processing. Indeed, time-domain measurement has numerous advantages over frequency-domain measurements. On the one hand, TD devices provide faster and simpler measurements because they use high-speed time sampling techniques and offer the possibility of capturing the signal in TD and compute its different spectral components in a shorter period (e.g., spectrum analyzers, which are more expensive than oscilloscopes, usually have a narrow resolution bandwidth). On the other hand, better precision is obtained using TD measurements because all the frequencies are simultaneously measured, mainly in the case of a one-time transient where only a single frequency is captured and in the case of a periodic signal (with repetitive events) where the frequency step could limit the identification of all the events of interest. In the literature, few TD-based works have been presented to obtain the different equivalent parameters of radiating sources [9–15]. In [11–13], authors have evaluated the performance of TD methods to deal with EM transients using a microstrip device. More studies have been performed in [11–14].

Nevertheless, these approaches select the frequency band, and complex calculations require powerful machines with sufficient memory [11]. In [10], the temporal electromagnetic inverse method has been developed and implemented using GA, and thus, it depends on initial GA options. Therefore, researchers have developed alternative TD methods based on electromagnetic time reversal (EMTR) for radiating source identification in literature. Indeed, several studies have been achieved in the field of electromagnetics using the time-reversal (TR) technique for different purposes such as in source location identification [14, 15], acoustics [16–18], and recently power electronics [19–27]. Several studies have demonstrated TR's robustness and efficiency [14, 27, 28]. However, a handful of studies investigated the use of TR for EMC applications in the time domain until now. Rachidi et al. have presented using electromagnetic time reversal in lighting location and faults detection in power networks [14].

Most of the existing TR studies dedicated to sources characterization have been applied in the far-field region [17, 19, 20]. While in the case of power electronic EM radiation measurement, a nearfield (NF) scan has proven to be more advantageous because it is less dependent on different test conditions such as application range and equipment. Recent studies, as in [3] and [10], report that different issues in the converter circuits, basically linked to transient disturbances with a quite short duration, should be investigated in the TD using an NF test bench. In [22, 23], the proposed method has been applied to identify the equivalent model of radiation of simple structure, as an interesting basic study but not representative enough to deal

with an advanced power circuit. Hence, this work applies the full time-domain method to a complicated board containing several bulky components with several radiating sources based on the electromagnetic time-reversal technique. Current and voltage high-speed commutations can create serious non-intentional transient disturbances covering a wide frequency band in structures such as power electronic converters. Knowing that in electromagnetic interferences (EMI) mitigation techniques (such as shielding), it is essential to predict radiating sources parameters at the early design stage to reduce emissions related to switching activities and parasitic interconnections. In this present work, we have studied the application of the EMTR technique based on time-domain analysis to reconstruct the radiation behavior and obtain an accurate equivalent model of the device under test (DUT), which emits critical non-sinusoidal signals. This methodology aims to help designers estimate radiated EM fields at different measurement distances and study the possible couplings between components.

Section 2 gives a detailed overview of the NF measurement test bench in the time domain. Moreover, the selected studied structure, which is an AC/DC flyback converter, is described. Section 3 discusses the theoretical investigations of the electromagnetic time-reversal technique and details the suggested implementation of the method for evaluating radiated emissions and sources reconstruction issues. Section 4 provides an application of the proposed EMTR-based method, and an adequate equivalent model that emits the same radiation behavior is studied.

Furthermore, a comparison study has been carried out for experimental validation purposes. The obtained results are presented in the form of time-dependent mappings of the magnetic nearfield. The last section outlines the main conclusions.

2. Time-domain measurements test bench

A TD test bench is employed to evaluate EM disturbances in the NF for power systems in this study. A single measurement (one scan) is carried out for multiples radiation frequencies at once.

2.1 TD measurement technique

TD measurement uses high precision measurement devices with a wide bandwidth, such as oscilloscopes, to capture temporal signals using a magnetic field probe. This measuring probe is nothing else than an academic small coil probe shielded sung copper [11] or a commercial magnetic loop of a radius equal to 1.6 mm generating a voltage from the varying magnetic flux. It scans the surface above the DUT, in the nearfield region, with a fixed displacement step, which prevents capacitive couplings and noise while measuring. The probe is connected to the scope using a shielded coaxial cable through an SMA connector, and it is calibrated as explained in [11, 29].

Indeed, based on the Faraday and Lenz laws and transformation equations, the variable magnetic field is obtained through the voltage measured at the terminals of the loop using the following equation:

$$H(t) = -\frac{1}{\mu_0 \times S} \int_0^t V(t)dt \tag{1}$$

Where $S = \pi \times r^2$, is the loop surface and $\mu_0 = 4 \times \pi \times 10^{-7}$ N/A^2 is the permeability in the free space.
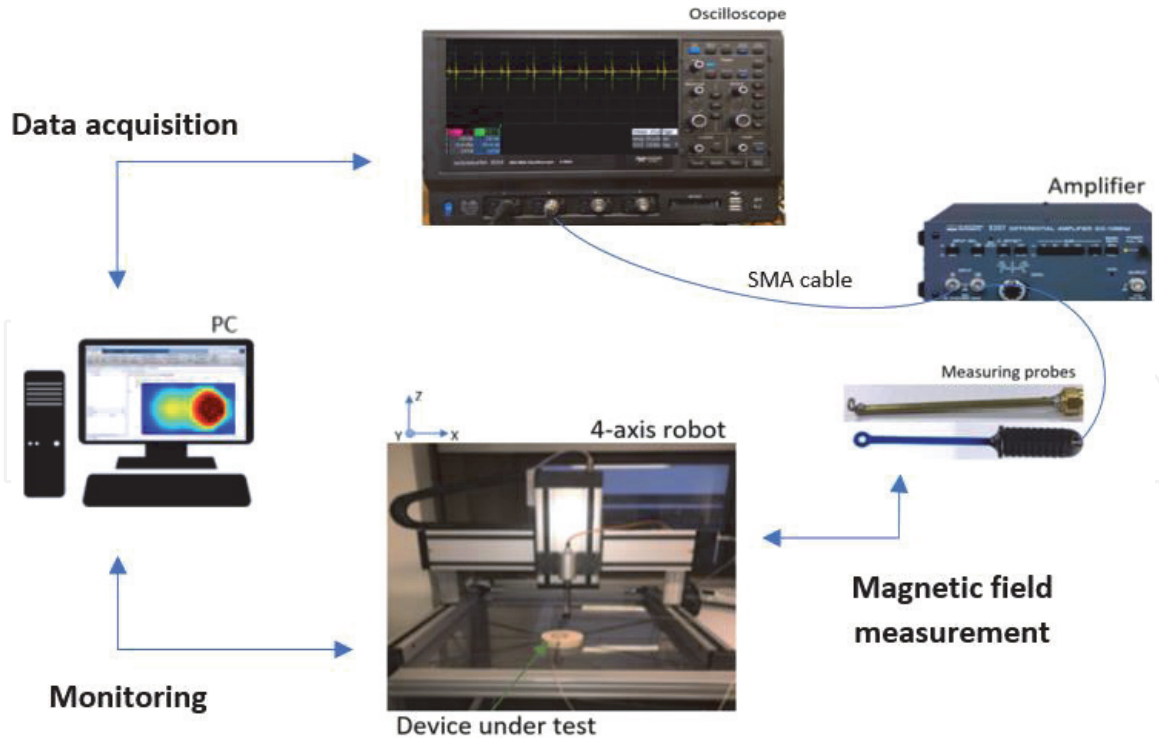
Figure 1.
Automated scanning test stands for NF measurement in the time domain.

The studied test bench provides a three-dimensional field measurement, but according to our needs, we only consider measuring the normal component of the magnetic field (H_z). Synchronous acquisitions are performed using a trigger, chosen to be a periodic and a repetitive reference signal. The following **Figure 1** presents the proposed nearfield test bench using a LeCroy WaveRunner 104XI oscilloscope.

2.2 Device under test: AC/DC flyback converter

In this work, the studied structure is a flyback AC/DC converter based on the principle of switched-mode power supplies (SMPS), as in [30]. Indeed, despite the superior efficiency that they can offer, these switching converters generate a lot of noise and EMI because of their high changing dv/dt and di/dt events. These power supplies have a complex structure regarding EM emissions. It generates different types of EMI, such as harmonics of switching frequency and high-frequency noise due to phase voltage ringing or the reverse recovery. In industry, this converter topology is typically used in both low and medium power as in automotive, battery charging and avionics, etc.

In practice, the design of the SMPS circuit is of great importance because it has to meet the configuration specifications in terms of energy storage and losses and avoid transient oscillations that generate EM interference modes covering a wide frequency band of several tens of MHz.

In our study, the DUT is a low power converter of 5 W. The top and bottom faces of the studied flyback AC/DC converter are shown in **Figure 2**. Its corresponding configuration parameters are presented in **Table 1**, and the schematic is depicted in **Figure 3**. To guarantee a synchronous acquisition, transient radiation signals at the scan surface have been measured with respect to the input of the optocoupler of the converter as a reference signal, **Figure 3**.

The NF radiation distribution of the DUT is obtained through a rigorous scan of the bottom face of the board, which allows avoiding bulky components and having a better recoding of EM emissions at a reasonable measuring distance.
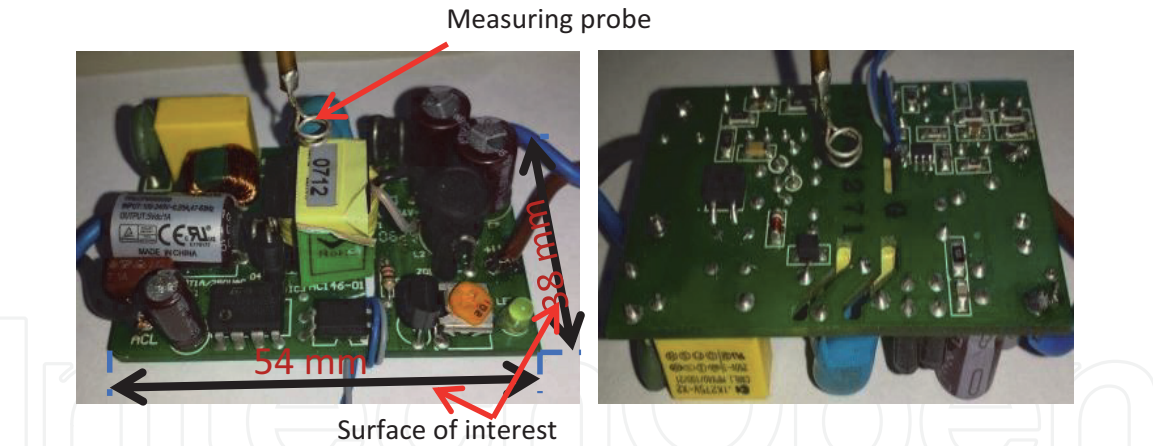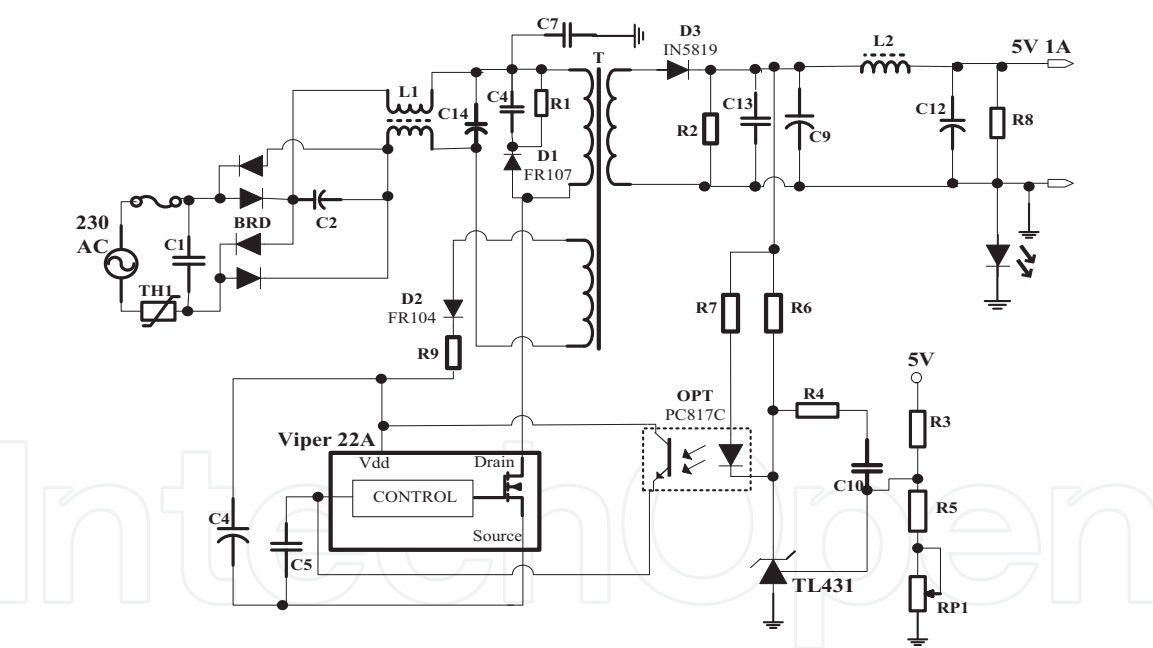
Figure 2.
Studied flyback AC/DC converter: top and bottom faces.

Input voltage	Output voltage	Switching frequency	Efficiency
220 V	5 V DC	60 kHz	79%

Table 1.
Parameters of the studied configuration.

Figure 3.
Schematic of the studied flyback AC/DC converter.

Scanning area	(**38 mm × 54 mm**)
Height of measurement	1.2 cm
Scanning resolution	2 mm
Scanning points	560 positions
Signals duration	20 µs

Table 2.
Measurement setup.

Figure 4.
Control signal.

Table 2 provides the measurement setup adopted in the present work, and **Figure 4** shows the control signal that ensures the smooth running of the converter.

A measured radiated signal is depicted in **Figure 5**. As we can notice in **Figure 6**, sources are not radiating simultaneously to obtain an intense radiation area at one time step but not in another. The radiation behavior of EM signals changes over time, and it is not evident to capture these events using frequency analysis only.

3. Basis of electromagnetic time-reversal technique

3.1 Theoretical principles

The time-reversal technique has been known for a long with great success in acoustics and ultrasound applications [17]. This has encouraged researchers to investigate the use of this method in the vast field of electrical engineering, such as in power line communications, fault location, and EMC issues [14, 15, 18–27]. Time and space focusing of waves is the specific feature of time-reversal theory [28]. Indeed, when a random source is in a pulse mode, generated signals are propagated indefinitely in the environment until they vanish (forward propagation). To measure these emissions, a set of transceivers is placed in a defined configuration called a time-reversal mirror (TRM). Then, recorded waves are time-reversed and injected into the same context (time reverse + back-propagation). After that, back-propagated waveforms will try to merge to form a maximum peak at a certain time step and position (focusing). In fact, the obtained location and parameters correspond to the actual source due to the reciprocity theorem and the reversibility in time of the wave equation. Hence, in an electromagnetic context, the performance of sources excited by high-frequency generators is easily evaluated or, more precisely, for an EMC
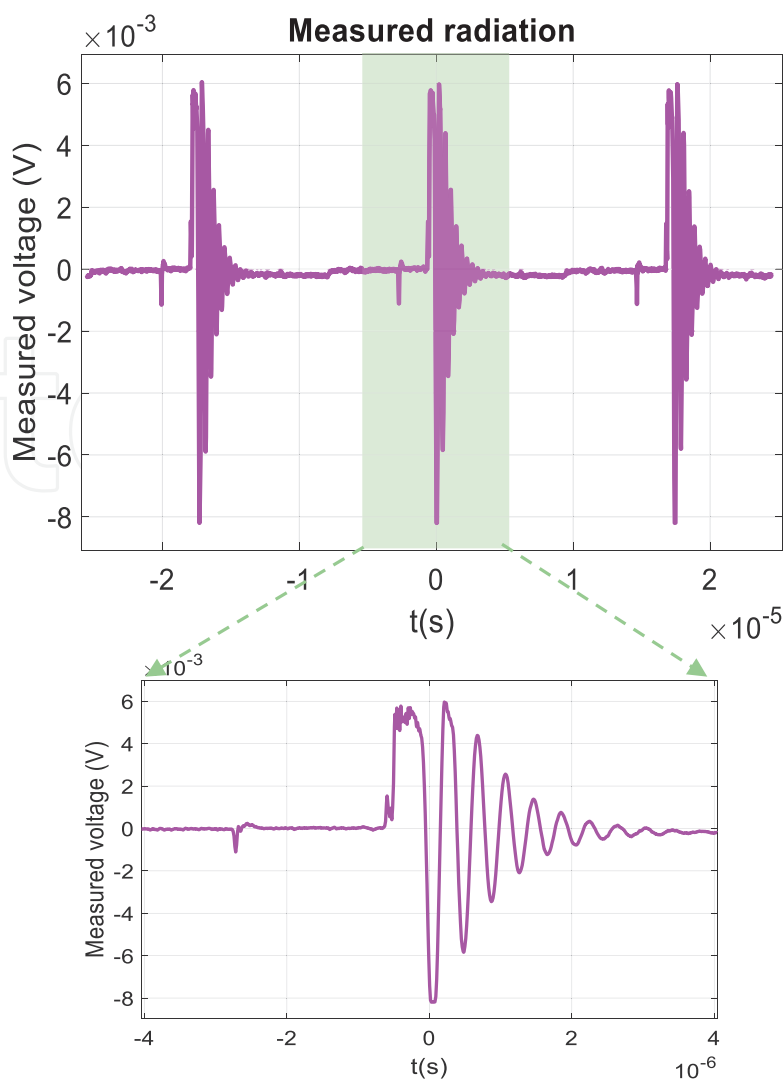
Figure 5.
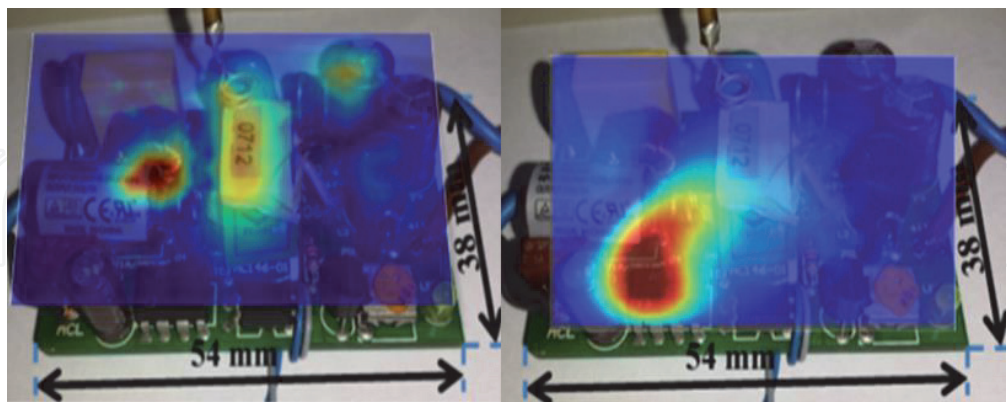*Captured waveforms: (a) whole signal, (b) window.*

Figure 6.
Measured radiation field maps above the DUT at two different time steps:$t_1 = 10.25$ μs and $t_2 = 10.5$ μs.

application. The EM emission behavior of a radiating source that exhibits high-level transients can be reconstructed in both space and time [14–27].

Based on the basic electromagnetic wave equations in a homogeneous medium, which is written as follows:

$$\frac{1}{c^2}\frac{\partial^2 \Phi}{\partial t^2} = \nabla^2 \Phi \tag{2}$$

Where Φ stands for electric E or magnetic H field, and c is the speed of light in free space.

If $f(t)$ is a solution of Eq. (1), then $g(t) = f(-t)$ is also a solution. In other words, theoretically, EM waves may propagate backward from the time step $t = T$ to $t = 0$ s. In practice, the measured magnetic (or electric) field $H(r,t)$ at probe position r and for each time step t, $t \in [0; T]$ where T is the time period and the back-propagated magnetic (or electric) field $H(r, T - t)$ are both solutions. However, it has been demonstrated that under the action of time inversion, the magnetic field H is of an odd parity [15, 31]. Accordingly, assuming that TR represents the time inversion operator, we have:

$$\text{TR}\{H(r,t)\} = -H(r,-t) \tag{3}$$

It is interesting to note that when a current $I(t)$ flows through a source, a magnetic field $H(t)$ is created. In the case of a conductive loop, the following relation gives the measured field:

$$H_i(t) = h(r_0 \rightarrow r_i, t) \otimes I(t) \tag{4}$$

Where $\otimes$ denotes a convolution product, $1 \leq i \leq N$ number of receiving antennas, and $h(r_0 \rightarrow r_i, t)$ is the impulse response of the system at a position r_i and for a pulse generated by r_0. Indeed, $h(t)$ represents the transfer matrix that rules the transmission and the reception procedures between the TRM transducers (area discretized into N positions) and a defined virtual set of point-like sources placed on the DUT surface and driven by a Dirac delta function. As a result, the focused signal is obtained as follows:

$$H_{TR}(r_0, t) = \sum_{i=1}^{N} h(r_i \rightarrow r_0, t) \otimes H_{x,y,z_i}(-t) \tag{5}$$

Where, $H_{TR}(r_0, t)$ represents the focused signal at the position r_0 and time step t. In the literature [14, 15], the excitation signal has commonly been identified as the reversed version of the extracted focusing signal at the source position r_0 using the following equation:

$$\text{Max}(r_0) = \max_{t \in T}(|H_{TR}(r_0, t)|) \tag{6}$$

3.2 Equivalent model determination

In power systems with high current levels, the magnetic field has a strong predominance effect. In the literature, particularly during the switching activity, disturbances resulting from high dI/dt and leading to a high-frequency current can occur. Thus, to model these transients, the inverse problem resolution has been proposed and applied to a nearfield scanning experiment. Indeed, an equivalent model in the nearfield region is defined as a set of equivalent dipoles that reproduce the same EM radiation behavior as the DUT. For an equivalent magnetic dipole, **Figure 1**, the main characteristics are the center position (X_d, Y_d, Z_d), orientation angles (θ, φ), diameter (the loop surface $S = \pi \times r^2$, where r is the radius), and the current I flowings in the loop [32]. The magnetic dipole moment M_d is the following:

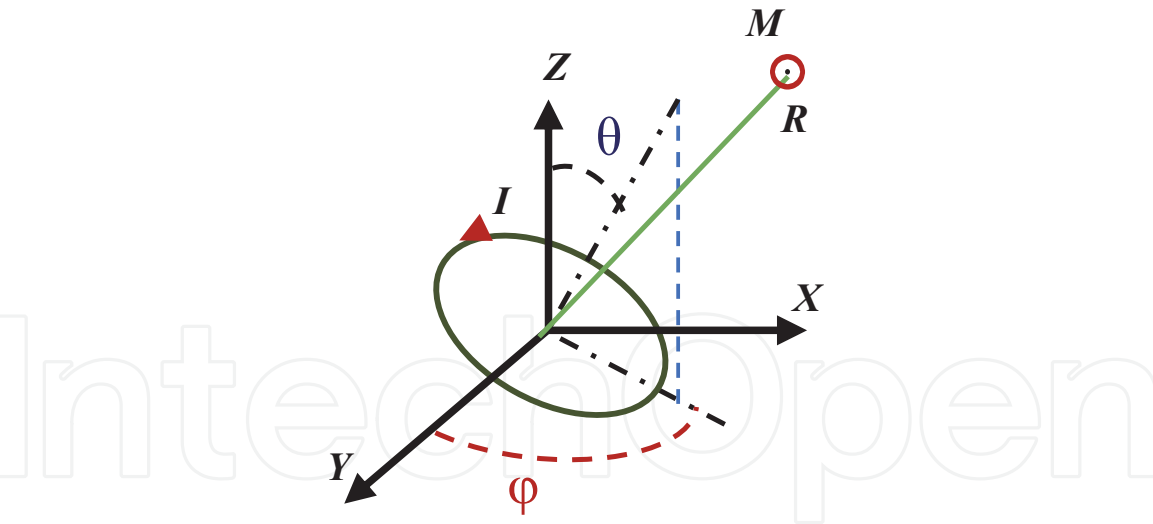$$\overrightarrow{M_d} = I \times \overrightarrow{S} \tag{7}$$

Figure 7.
Definition of an equivalent magnetic dipole.

From the formula for the equivalent field radiated by a magnetic loop in the nearfield, expressed by (8), we can obtain the three-dimensional distribution map of the radiated field (H_x, H_y and H_z) in a defined height of measurement using a time-domain representation (**Figure 7**).

$$H_{x,y,z} = A\left[(B_1 C_{x,y,z}) - (B_3 D_{x,y,z} E) \right] \tag{8}$$

Where:

$$A = \frac{1}{4\pi R} \tag{9}$$

$$B_{m=1,3} = \left(\left(\frac{1}{c^2} \frac{\partial^2 M_d(t')}{\partial t^2} \right) + \left(\frac{m}{cR} \frac{\partial M_d(t')}{\partial t} \right) + \left(\frac{1}{R^2} M_d(t') \right) \right) \tag{10}$$

$$C_{x,y,z} = (\sin(\theta)\cos(\varphi), \sin(\theta)\sin(\varphi), \cos\theta) \tag{11}$$

$$D_{x,y,z} = \frac{1}{R^2} ((X_d - X_0), (Y_d - Y_0), (Z_d - Z_0)) \tag{12}$$

$$E = \begin{pmatrix} \cos(\theta)(Z_d - Z_0) + \\ \sin(\theta)\sin(\varphi)(Y_d - Y_0) + \\ \sin(\theta)\cos(\varphi)(X_d - X_0) \end{pmatrix} \tag{13}$$

$$R = \sqrt{(X_d - X_0)^2 + (Y_d - Y_0)^2 + (Z_d - Z_0)^2} \tag{14}$$

$$t' = t - \frac{R}{c} \tag{15}$$

3.3 Applying EMTR to radiating source identification

This work focuses on the characterization of EM emissions in the nearfield using an equivalent radiation model. An algorithm based on electromagnetic time-reversal technique is applied to identify radiating sources parameters using the time-domain analysis. Indeed, in practice, active sources are not radiating
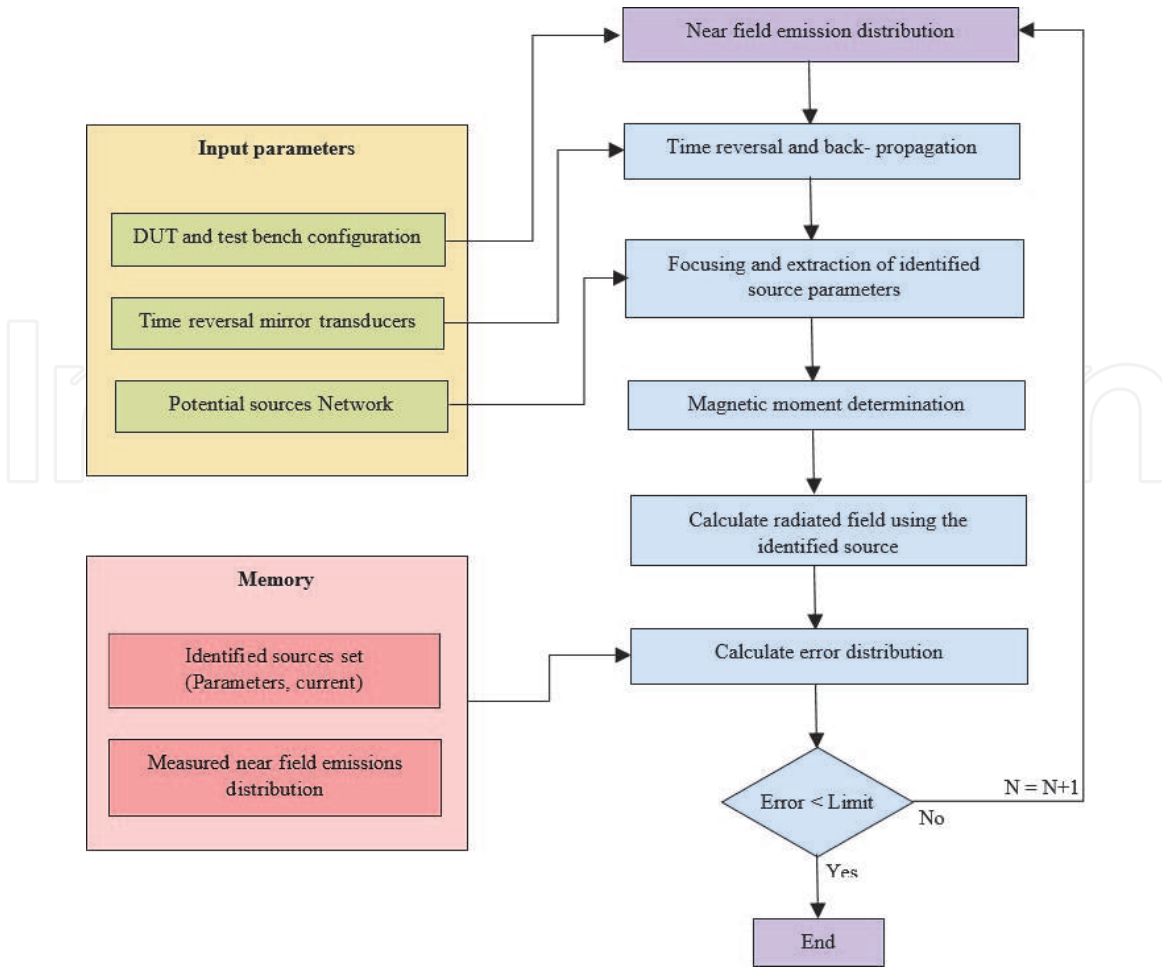
Figure 8.
Flowchart of the proposed method based on the EMTR technique.

simultaneously and the emission distribution at each time step corresponds only to the contributions of the different sources at this specific time. In the proposed method, an elimination process is carried out over time, starting from the most radiating sources (a hot spot in the map where the radiation level is significantly greater than the neighboring regions in the scanning area), using (5) and (6). A reconstructed field distribution is obtained using the identified source parameters, Eq. (8). Then, the difference between the measured and the estimated scans is evaluated using an error distribution at each iteration. To guarantee the convergence of the method and obtain a physical meaning model, an error limit is defined as a threshold value. Ideally, the estimated scan corresponds to the measured one, and then, the error limit equals zero. Apart from that, as in an NF experiment, the threshold corresponds to the measurement errors magnitudes (can be estimated when making measurement tests without a load). The effect of the different configuration parameters involved in this method has been studied in [33]. The flowchart of the whole procedure is shown in **Figure 8**.

4. Application of the proposed method

4.1 Modeling of the flyback converter

An adequate equivalent radiation model has been identified by applying the proposed EMTR method to the measured emissions of the AC-DC converter

N	Max moment $(A \times m^2) \times e - 7$	Coordinates (mm)			Orientations (rad)	
# 1	0.1545	10.9;	11.6;	− 0.67	0	1, 5708
# 2	0.2477	5 e − 3;	2 e − 2;	0.0	0	0
# 3	0.0708	−2.7;	− 11.6;	− 0.7	0	−1, 5708
# 4	0.0163	5.4;	− 15.4;	− 1.2	1, 5708	1, 5708
# 5	0.0900	13.6;	− 3.8;	− 0.37	1.5708	0
# 6	0.0179	−5.4;	3.9;	0.0	0	0
# 7	0.3468	13.6;	− 7.7;	− 0.61	0	1, 5708

Table 3.
THE Obtained equivalent model parameters.
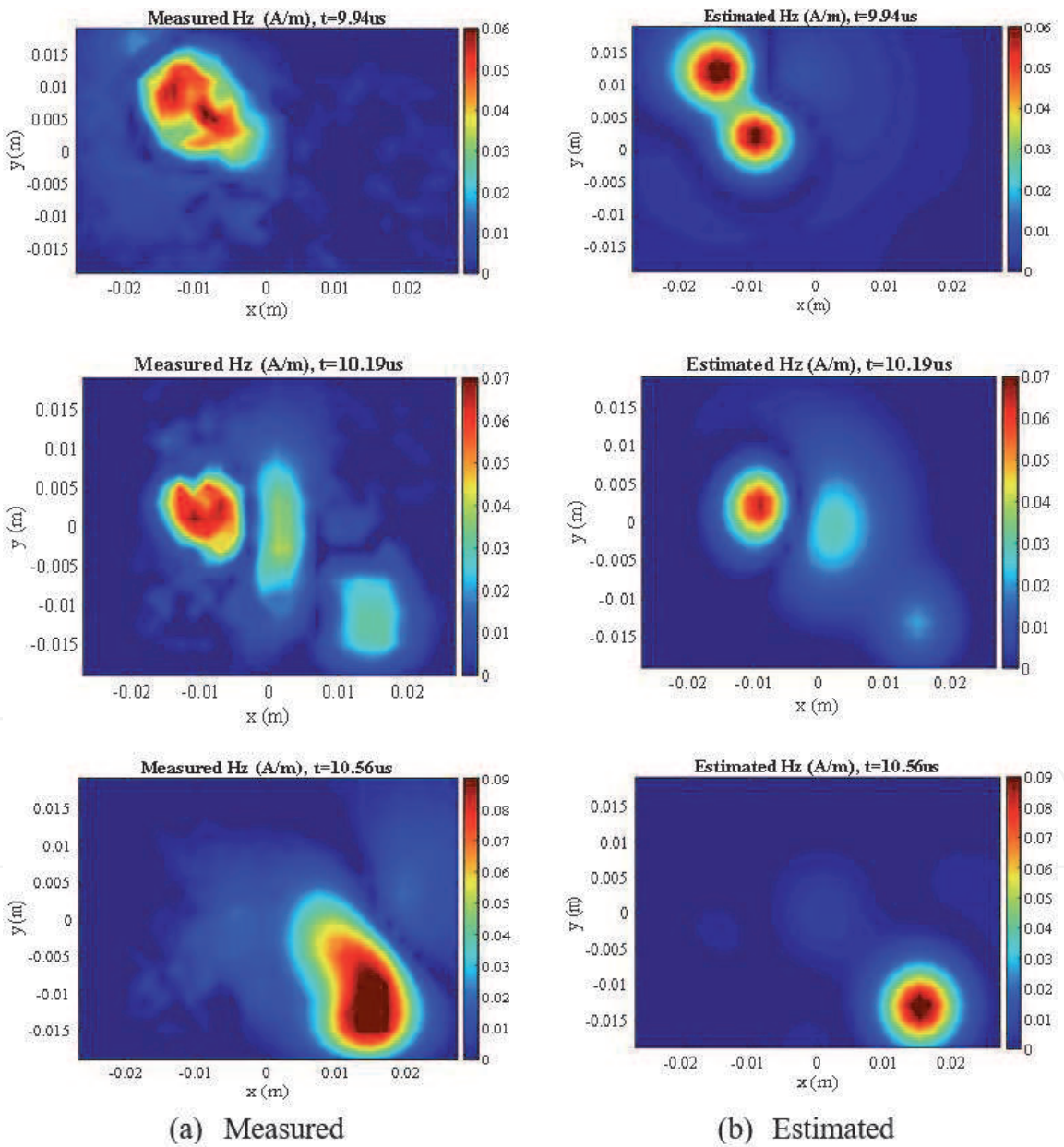

(a) Measured (b) Estimated

Figure 9.
Magnetic nearfield maps of z-component in TD: (a) measured. (b) Estimated.

obtained, as previously explained. Indeed, by comparing measured and estimated magnetic nearfield distribution H_z, using identified sources parameters given in **Table 3**, at a constant height of measurement and scan area, we can notice a good
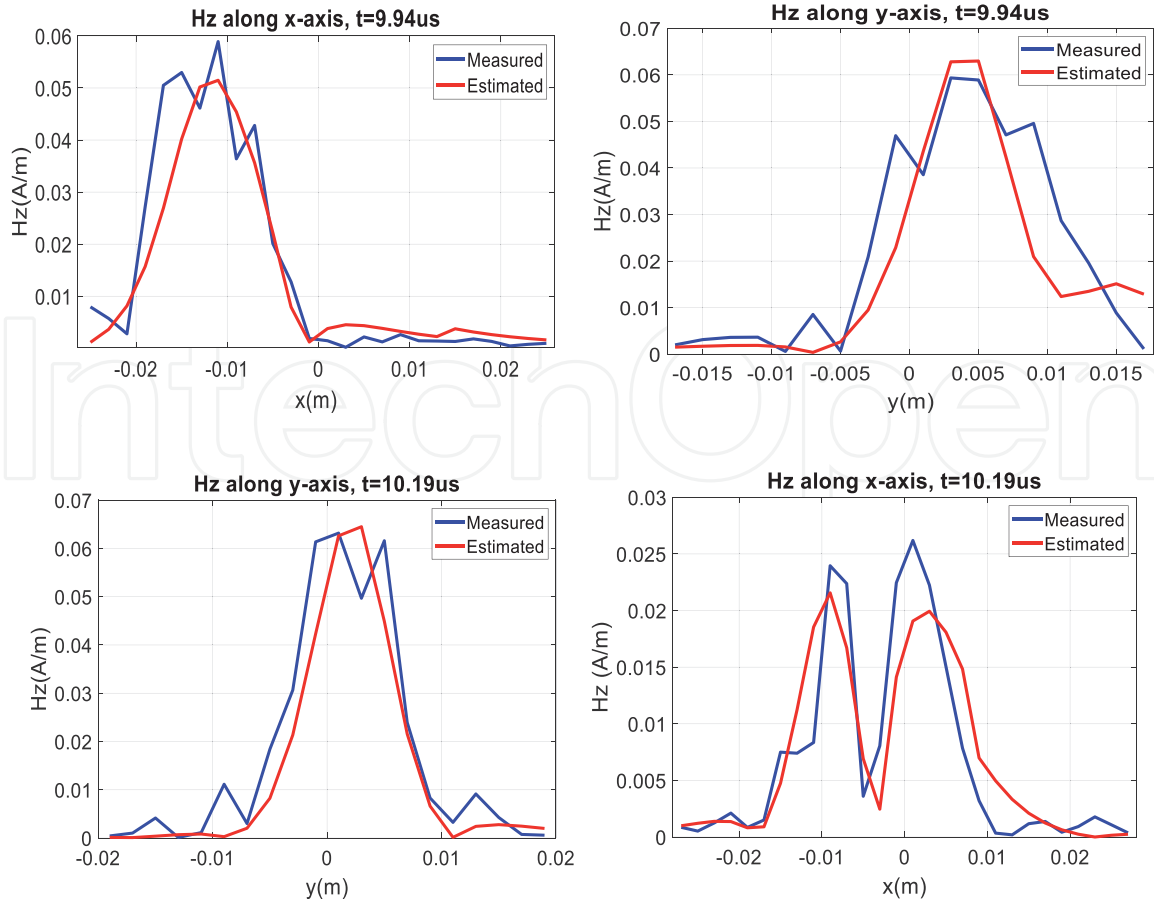
Figure 10.
Cuts of measured and simulated H_z at $Z = 0$.

agreement between the two sets of results along time, as shown in **Figure 9**. Particularly, the obtained equivalent sources perform valid waveforms with less noise as if they have been captured when scanning the circuit without measurement errors (which is inevitable in practice).

In **Figure 10**, estimated radiated field cuts at $Z = 0$ are compared to the reference signals along the x- and y-axis. Moreover, besides H_z reconstruction, the prediction of H_x and H_y is easy by including the obtained sources parameters in the analytical expressions of the magnetic field, as in (8).

It is worth noting that in order to the enhance the obtained results, it would be great to refine the mesh of the scanning area further and reduce even more the error limit (corresponding to the measurement errors including the test stand inaccuracies, spatial probe motion, and the coupling effects between the probe and the DUT, etc.). Nevertheless, both a large memory and a considerable computing time are needed.

4.2 Validation of the obtained model

In this study, we propose to confirm the efficiency of the obtained results using the EMTR-based method in TD with a standard inverse method performed in the frequency domain. Thus, we do not make measurements using an FD test bench, but we instead proceed by applying a fast Fourier transform to the measured magnetic field signals in TD. Indeed, in **Figure 11**, we notice the existence of several harmonics covering tens of megahertz in the frequency spectrum of the obtained FD magnetic field at different probe positions. This is among the major
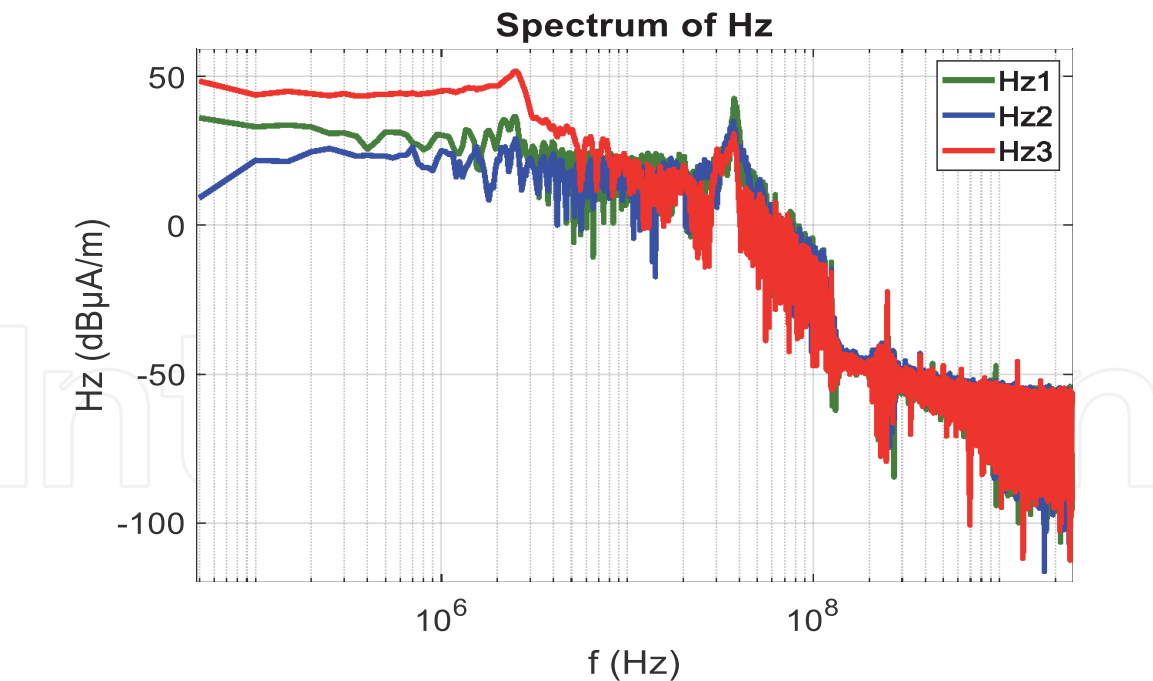
Figure 11.
The spectrum of the measured magnetic field above DUT at different positions.

disadvantages of FD measurements, especially in multisource structures with different characteristics and radiation patterns. We have implemented an optimization method based on genetic algorithms to apply the frequency inverse method and obtain an equivalent model for each studied frequency [8, 9]. In fact, the iterative process needed in this procedure can be reduced when choosing only significant frequencies; otherwise, it is time and memory-consuming. Moreover, to guarantee and accelerate the convergence of the method, a fine configuration has to be employed, particularly having a proper choice of the variable boundaries and population size. In **Figure 12**, mappings of the measured and estimated radiated field are depicted for different frequencies.

A good agreement is achieved between FD maps of measured fields and estimated using an optimization algorithm at different frequencies. Similar source positions have been obtained, which confirms the previous results. Looking at **Figures 9** and **12**, we notice that the proposed method based on EMTR matches the measurements better. Indeed, TD investigations provide rapid results, making modeling easier to use in critical test cases. It is worth noting that FD maps are only depicted at a single frequency for each measurement, and then, we cannot observe the behavior of all existing radiating sources without performing several measurement tests. However, a single temporal measurement is required for a TD method, as we have explained.

For further validation purposes, we propose to reconstruct the x-component of the EM field (H_x) using the obtained equivalent model and then compare the generated maps to the measured radiation distributions acquired with the magnetic probe dedicated for tangential components capturing. **Figure 13** shows an example of mappings at a defined time step. A good agreement is noticed between measured and estimated H_x. Hence, we conclude that the obtained equivalent magnetic dipoles are in good positions and that the proposed method is efficient in providing an equivalent method reproducing a three-dimensional reconstruction of the radiated field describing the overall behavior of the studied converter.
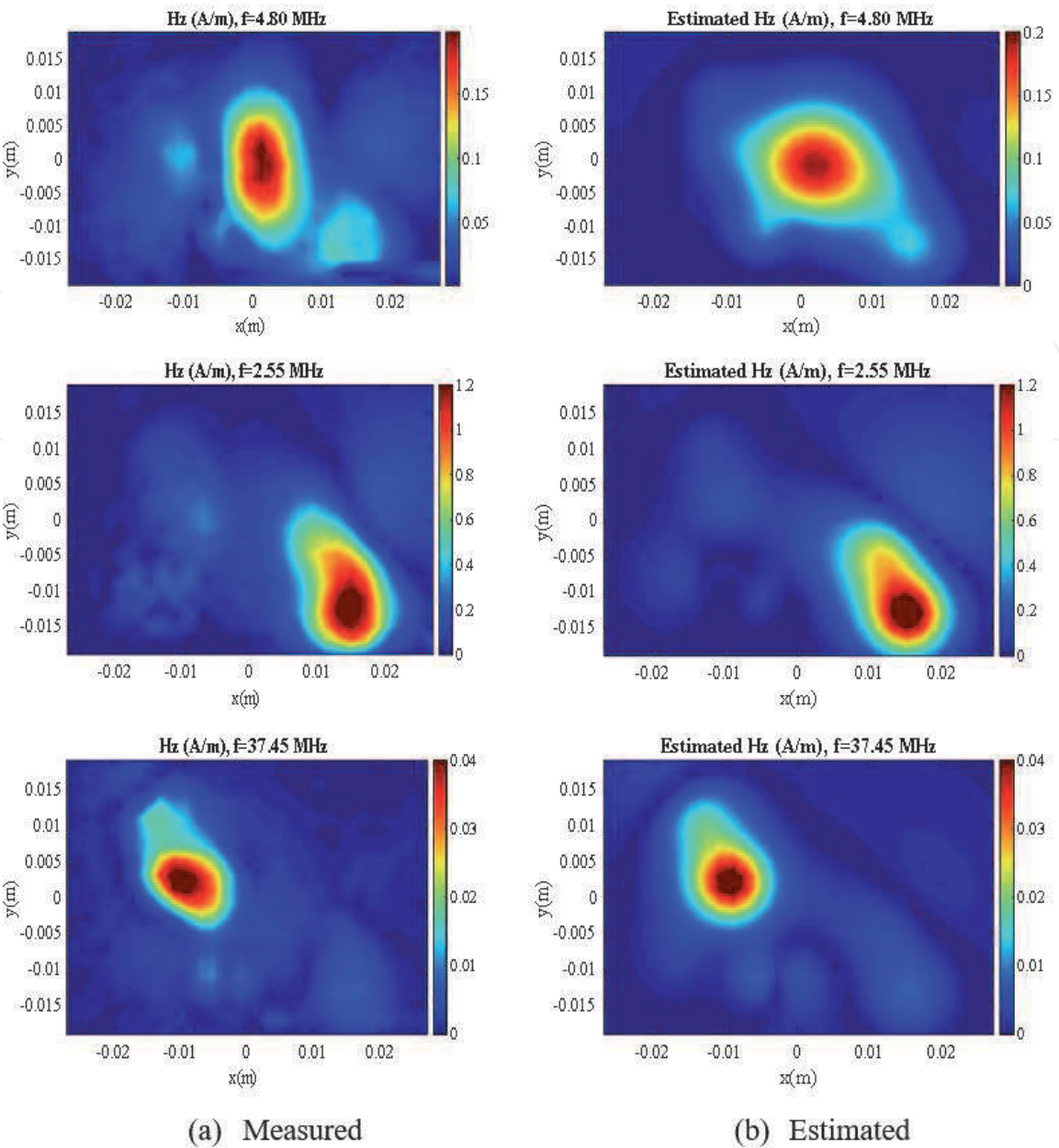
(a) Measured   (b) Estimated

Figure 12.
Magnetic NF maps of z-component in FD: (a) measured. (b) Estimated.
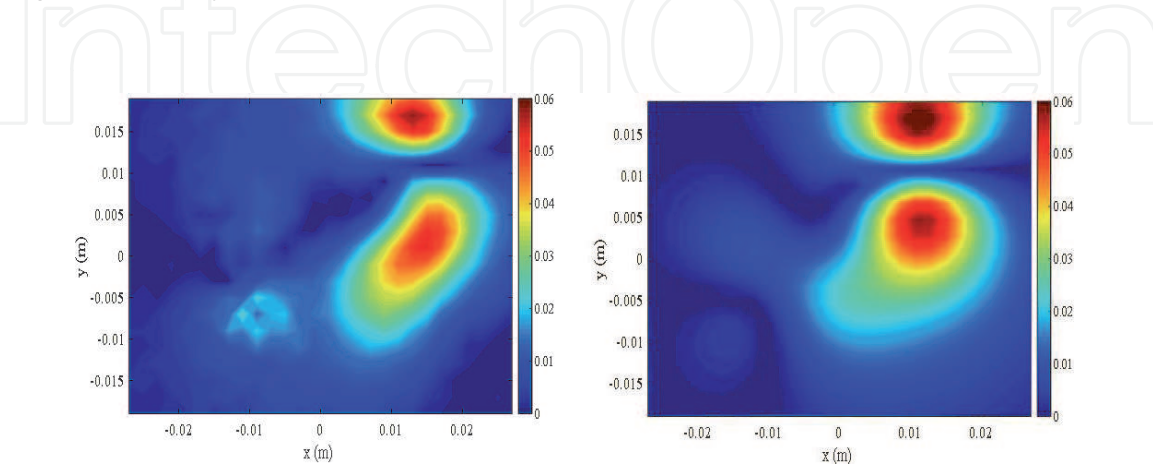

Figure 13.
Measured and estimated magnetic NF maps of x-component at t = 10.50 μs.

5. Conclusion

The motivation of the presented work was the characterization of electromagnetic radiating sources commonly found in power converter circuits. Time-domain measurement of the radiated field has been carried out in the nearfield using a specific test bench, including high-precision tools. An electromagnetic inverse method based on the EMTR technique has been studied to obtain an efficient equivalent model of the device under test. In case of transient disturbances that occur, for instance, during the turn-on of the transistor of a flyback AC/DC converter, a satisfactory agreement has been achieved between measured and estimated radiation maps, along with a reasonable computation time and memory usage. By comparing these results to a standard frequency domain inverse method based on the genetic algorithm, the proposed TD method has been shown to be advantageous over the FD method for EMC studies and to deal with related EMI issues in advanced electronic systems such as in power electronics and those developed for avionics and wireless communication. Furthermore, we conclude that the EMTR-based method is a good alternative for studying electromagnetic radiation behavior with a three-dimensional reconstruction in the case of multisource structures.

Author details

Sassia Hedia[1,2,3]*, Bessem Zitouna[1], Jaleleddine Ben Hadj Slama[1]
and Lionel Pichon[2,3]

1 LATIS, Laboratory of Advanced Technology and Intelligent Systems, ENISo, National Engineering School of Sousse, University of Sousse, Tunisia

2 Group of Electrical Engineering-Paris, CNRS, CentraleSupélec, Université Paris-Saclay, Gif-sur-Yvette, France

3 Group of Electrical Engineering-Paris, CNRS, Sorbonne Université, CNRS, Paris, France

*Address all correspondence to: hdia.sassia@gmail.com

IntechOpen

References

[1] Clayton RP. *Introduction to Electromagnetic Compatibility*. Vol. 184. Hoboken, NJ, USA: Wiley, 2006

[2] Beghou L, Costa F, Pichon L. Detection of electromagnetic radiations sources at the switching time scale using an inverse problem-based resolution method—application to power electronic circuits. IEEE Transactions on Electromagnetic Compatibility. 2015; **57**(1):52-60

[3] Vives-Gilabert Y, Arcambal C, Louis A, de Daran F, Eudeline P, Mazari B. Modeling magnetic radiations of electronic circuits using near-field scanning method. IEEE Transactions on Electromagnetic Compatibility. 2007; **49**(2):391-400

[4] Essakhi B et al. Characterization of radiated emissions from power electronic devices: synthesis of an equivalent model from nearfield measurement. The European Physical Journal-Applied Physics. 2007;**38**(3): 275-281

[5] Shall H, Riah Z, Kadi M. A 3-D near-field modeling approach for electromagnetic interference prediction. IEEE Transactions on Electromagnetic Compatibility. 2014; **56**(1):102-112

[6] Benyoubi F, Pichon L, Bensetti M, Le Bihan Y, Feliachi M. An efficient method for modeling the magnetic field emissions of power electronic equipment from magnetic near field measurements. IEEE Transactions on Electromagnetic Compatibility. 2017; **59**(2):609-617

[7] Saidi S, Ben Hadj Slama J. A near-field technique based on PZMI, GA, and ANN: application to power electronics systems. IEEE Transactions on Electromagnetic Compatibility. 2014; **56**(4):784-791

[8] Sivaraman N. *Design of Magnetic Probes for Near Field Measurements and the Development of Algorithms for the Prediction of EMC*. Diss: Université Grenoble Alpes; 2017

[9] Ravelo B, Yang L. Computation of transient nearfield radiated by electronic devices from frequency data. In: Fourier Transform Applications. Rijeka: InTech; 2012

[10] Zitouna B, Ben Hadj Slama J. Enhancement of time-domain electromagnetic inverse method for modeling circuits radiations. IEEE Transactions on Electromagnetic Compatibility. 2016;**58**(2):534-542

[11] Liu Y, Ravelo B. Fully time-domain scanning of EM nearfield radiated by RF circuits. Progress In Electromagnetics Research. 2014;**57**:21-46

[12] Liu Y, Ravelo B, Jastrzebski AK. Time-domain magnetic dipole model of PCB nearfield emission. IEEE Transactions on Electromagnetic Compatibility. 2016;**58**(5):1561-1569

[13] Ravelo B, Liu Y, Jastrzebski AK. PCB near-field transient emission time-domain model. IEEE Transactions on Electromagnetic Compatibility. 2015; **57**(6):1320-1328

[14] Rachidi F. Rubinstein M, Paolone M. Electromagnetic Time Reversal: Application to Electromagnetic Compatibility and Power Systems. Hoboken, NJ, USA: Wiley; 2017

[15] El Baba I, Lalléchère S, Bonnet P. Electromagnetic time-reversal for reverberation chamber applications using FDTD, Proceedings of ACTEA 2009, International Conference on Advances in Computational Tools for Engineering Applications, Lebanon; 2009. pp. 157-167, ISBN: 978-1-4244-3833-4

[16] Fink M. Time reversal of ultrasonic fields. I. Basic principles. IEEE Transactions on Ultrasonics, Ferroelectrics, and Frequency Control. Sept. 1992;**39**(5):555-566

[17] Minonzio J, Davy M, de Rosny J, Prada C, Fink M. Theory of the time-reversal operator for a dielectric cylinder using separate transmit and receive arrays. IEEE Transactions on Antennas and Propagation. 2009;**57**(8):2331-2340

[18] Conti SG, Roux P, Kuperman WA. Nearfield time-reversal amplification. The Journal of the Acoustical Society of America. 2007;**121**(6):3602-3606

[19] Wang Z et al. A full-scale experimental validation of electromagnetic time reversal applied to locate disturbances in overhead power distribution lines. IEEE Transactions on Electromagnetic Compatibility. 2018;**60**(5):1562-1570

[20] Spirlet M, Broun V, Camus P, Geuzaine C, Beauvois V, Molenberg I. Modelling time reversal applications in a reverberation chamber using the current image method. In: 2013 International Symposium on Electromagnetic Compatibility, Brugge. 2013. pp. 359-364

[21] Kosmas P, Rappaport CM. FDTD-based time reversal for microwave breast cancer detection-localization in three dimensions. IEEE Transactions on Microwave Theory and Techniques. 2006;**54**(4):1921-1927

[22] Hedia S, Zitouna B, Ben Hadj Slama J, Pichon L. Electromagnetic time reversal for radiating source identification in time domain. In: *2018 15th International Multi-Conference on Systems, Signals & Devices (SSD)*, Yassmine Hammamet, Tunisia. 2018. pp. 531-536

[23] Hedia S, Zitouna B, Ben Hadj Slama J, Pichon L. A full time domain methodology based on near field time reversal for equivalent source identification. In: 2018 IEEE International Symposium on Electromagnetic Compatibility and 2018 IEEE Asia-Pacific Symposium on Electromagnetic Compatibility (EMC/APEMC), Singapore. 2018. pp. 141-146

[24] El Baba I, Lalléchère S, Bonnet P. Time reversal for electromagnetism: applications in electromagnetic compatibility. Trends in Electromagnetism: From Fundamentals to Applications. 2012;**177**:177-206

[25] Ungureanu A, Vuong TP, Ndagijimana F. Electromagnetic point source reconstruction by reversed-TLM method. Applied Computational Electromagnetics Society Journal. 2011;**26**(9):754-759

[26] Chabalko MJ, Sample AP. Electromagnetic time reversal focusing of near field waves in metamaterials. Applied Physics Letters. 2016;**109**(26):263901

[27] De Rosny J, Lerosey G, Fink M. Theory of electromagnetic time-reversal mirrors. IEEE Transactions on Antennas and Propagation. Oct. 2010;**58**(10):3139-3149

[28] De Rosny J, Fink M. Focusing properties of nearfield time reversal. Physical Review A. 2007;**76**(6):065801

[29] Benyoubi F, Feliachi M, Le Bihan Y, Bensetti M, Pichon L. Implementation of tools for electromagnetic compatibility studies in the near field. In: *International Conference on Electrical Sciences and Technologies in Maghreb (CISTEM)*, Marrakech. 2016. pp. 1-6

[30] Zitouna B, Ben Hadj Slama J. Time domain inverse method based on the near field technique to solve electromagnetic interference problems: Application to an AC/DC flyback

converter. IET Power Electronics. 2018;
11(13):2133-2139

[31] Jackson JD. Classical
Electrodynamics. Hoboken, New Jersey,
USA: John Wiley & Sons; 1999.
pp. 841-842

[32] Balanis CA. Antenna Theory:
Analysis & Design. Hoboken, NJ, USA:
Wiley, 1997

[33] Hedia S, Zitouna B, Ben Hadj
Slama J, Pichon L. Characterization of
radiating sources in the NEAR field using
EMTR technique: A parametric study. In:
2020 6th IEEE International Energy
Conference (ENERGYCon). 2020.
pp. 104-109